Estudios Geol., 56: 3-18 (2000)

TRIASSIC THOLEIITIC DOLERITES («OPHITES») OF THE EL GRADO DIAPIR (PYRENEES, HUESCA, SPAIN): EMPLACEMENT AND COMPOSITION

M. Lago San José *, C. Galé Bornao *, E. Arranz Yagüe *, R. Vaquer Navarro **, A. Gil Imaz * y A. Pocovi Juan *

ABSTRACT

Mesozoic dolerites in the south Pyrenean sector of El Grado (Huesca, Spain) preserve emplacement structures (fluidity structures at the top and load structures at the base) developed during their intrusion into unconsolidated marly-evaporitic Triassic sediments (Keuper facies). By analogy with other dolerites in the south Pyrenean domain, their emplacement age is equivalent to the uppermost Keuper facies terms, but prior to the final Triassic-early Liassic carbonated sediments. Radiometric ages (187-197±7 Ma) show that the emplacement occurred during the lower Liassic.

The petrological differentiation from the chilled margin facies to the central facies, and also to the late pegmatitoids, is consistent with that obtained from major elements, trace elements and REE. Their tholeiitic affinity, as defined by their geochemical composition, is equivalent to that of similar rocks in the Pyrenean domain. However, the rocks analyzed here, which are located at the external sector of this domain, display a greater petrological and geochemical differentiation as compared to similar rocks in the central sectors of the Pyrenean domain.

Key words: *dolerites, tholeiitic composition, emplacement, radiometric age, Pyrenean domain.*

RESUMEN

Las doleritas mesozoicas del sector surpirenaico de El Grado (Huesca) conservan estructuras de emplazamiento (con desarrollo del movimiento de lava fluida al techo y de carga en su base) desarrolladas al instruir en los sedimentos margo-evaporíticos en facies Keuper, todavía inconsolidados. Por similitud con otras doleritas del dominio surpirenaico, la edad del emplazamiento es equivalente a la de los términos superiores de la facies Keuper y previa a la sedimentación carbonatada del Trías terminal-Lías inferior. Las determinaciones de edades radiométricas (187-197±7 Ma) indican que el emplazamiento debió tener lugar durante el Lías inferior.

La diferenciación petrológica, desde la facies del borde enfriado a la central y, también, al posterior diferenciado pegmatoide concuerda con la obtenida con elementos mayores, trazas y REE. Su afinidad toleítica, definida por su composición geoquímica, coincide con la obtenida en rocas análogas para el dominio pirenaico; no obstante, estas rocas situadas en el borde más externo de dicho dominio representan una mayor diferenciación (petrológica y geoquímica) respecto a la obtenida, hasta el momento, para rocas análogas situadas en sectores más centrales del citado dominio pirenaico.

Palabras clave: *doleritas, composición toleítica, emplazamiento, edad radiométrica, dominio Pirenaico.*

Introduction

The Triassic tholeiitic dolerites («ophites») of the El Grado diapir (Huesca, Spain) preserve the main features of a subvolcanic emplacement mechanism, and constitute a useful reference in the study of this type of magmatism, which is widely represented in the Pyrenean domain

* Departamento de Ciencias de la Tierra. Universidad de Zaragoza. 50009 Zaragoza (Spain).
** Departamento de Geoquímica, Petrologia i Prospecció Geològica. Zona Universitària de Pedralbes. 08071 Barcelona (Spain).

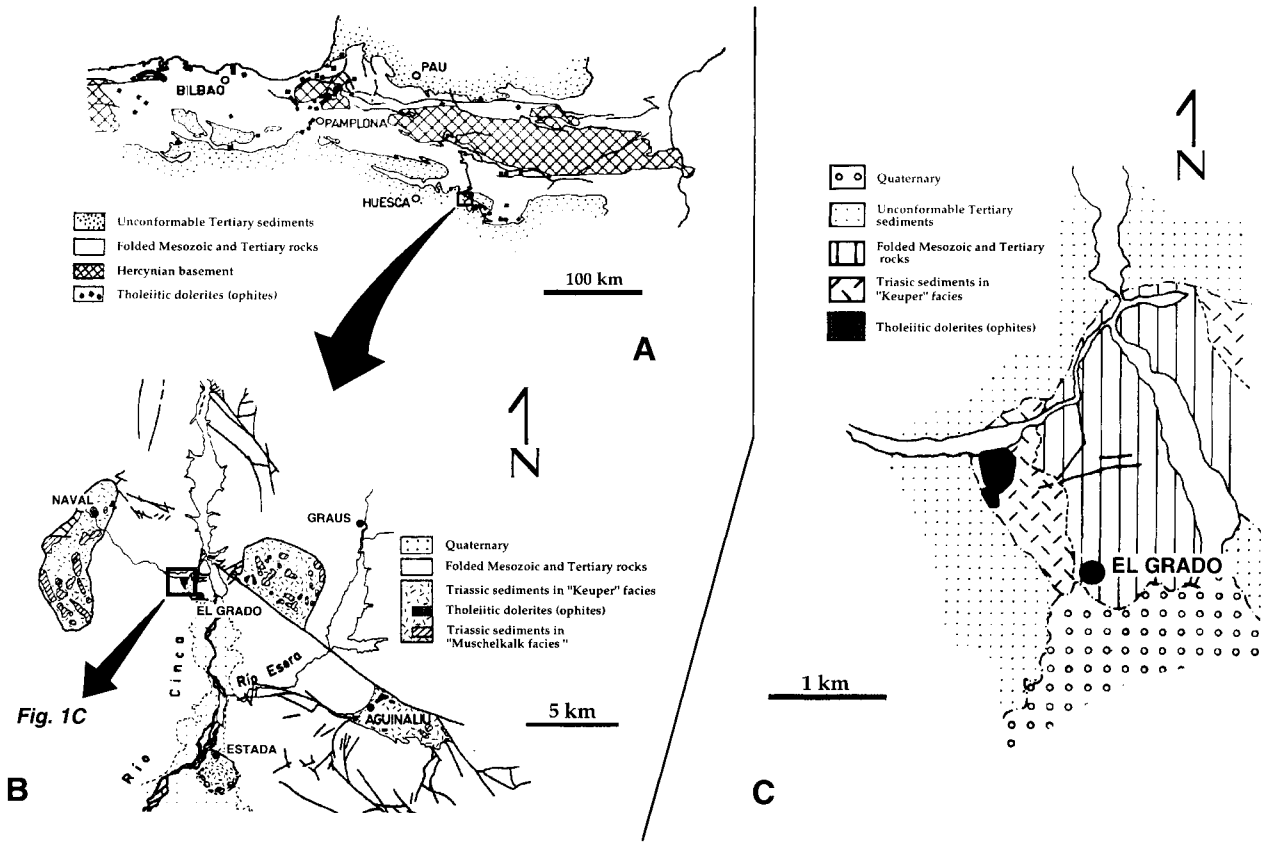

Fig. 1.—Geological setting of the studied area: Global setting of th Pyrenean chain (A); Geological sketch of the area (B); Geological sketch of the El Grado diapir (C).

(fig. 1A). These dolerites, which outcrop as two sills, show a series of ideal characteristics for their study: 1) the present exceptionally well preserved fluidity structures, 2) they induced a very low grade contact metamorphism on their hosting sediments and 3) the three well represented rock-types (chilled margin, central facies and pegmatitoid [1] differentiate) display mineralogical and geochemical compositions typical of this magmatism and its crystallization conditions. In this sense, the El Grado ophites are even more interesting than the Estopiñán and Laredo outcrops (Pyreneean tholeiitic peri-atlantic domain) which were used as references for this type of magmatism in the Pyrenees (Lago & Pocovi, 1982 and 1984).

Finally, our paper offers new data on the mineral composition evolution of dolerites, specially in their late stages (amphiboles and biotites), as well as more comprehensive geochemical data regarding the dolerites of the south Pyrenean domain (major, trace elements and REE).

Geological setting, age and emplacement conditions

The dolerite outcrop of the El Grado diapir (figs. 1B and 1C), was emplaced within marly-evaporitic sediments of the Triassic Keuper facies. This diapir belongs to a lineation of diapirs connecting the «Sierras Marginales Aragonesas» and the «Sierras Marginales Catalanes» (Martínez & Pocovi, 1988). Two different kinds of processes were involved in this diapirism: 1) piercing of the Mesozoic and Tertiary cover in anticlinal cores and thrust fronts, and 2) diapir development by halokinesis of Late Triassic evaporitic sediments. The former process belongs to the Pyrenean tectogenesis, characterized by folding and sliding of cover materials towards the south, to form a complex thrusting sequence during the Late Eocene-Oligocene (Martínez, 1982; Cámara & Klimowitz, 1985; Martínez & Pocovi, 1988). The later represents the rise of plastic and less dense materials from zones where they had concentrated during the first pro-

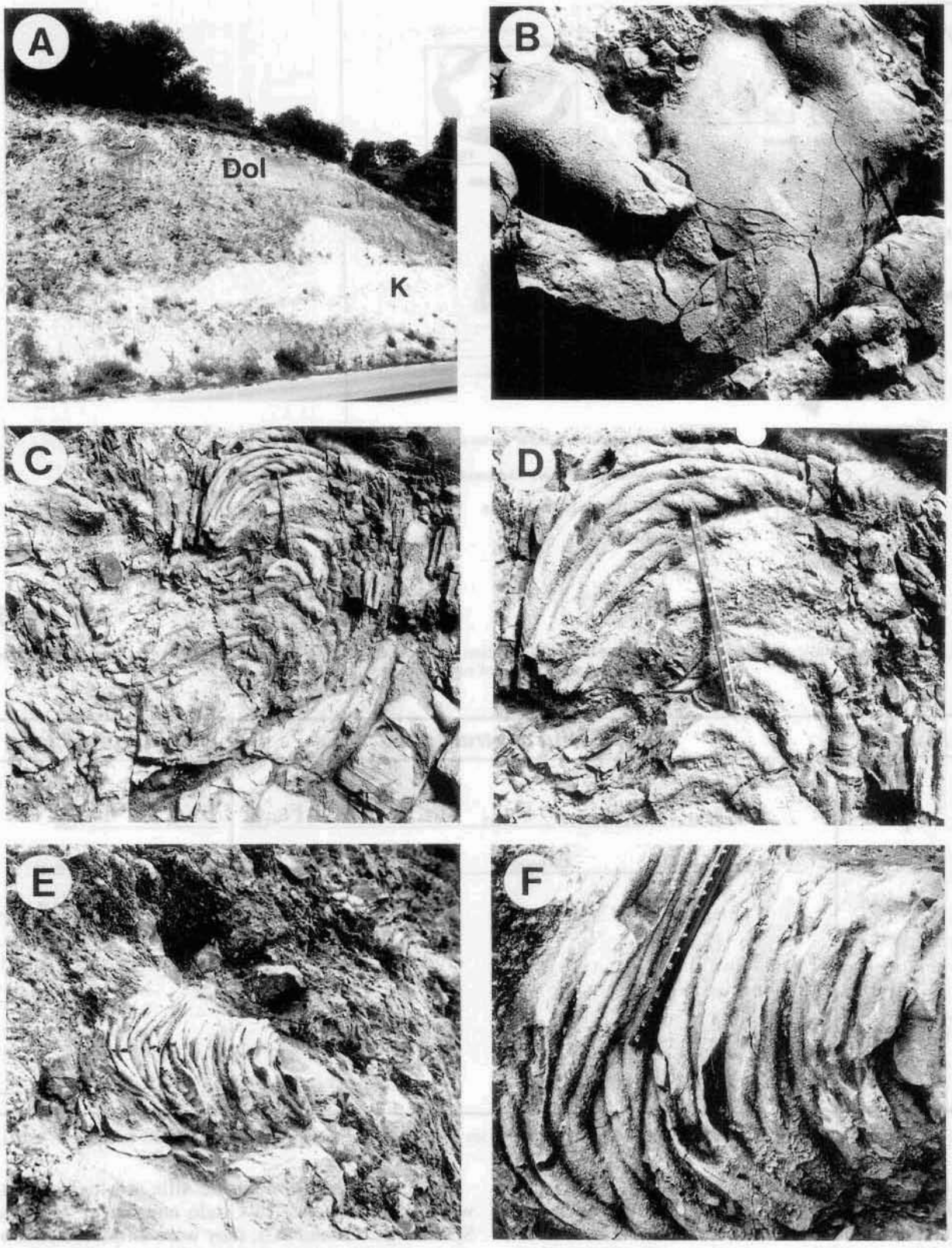

Fig. 2.—(A): Outcrop section showing hosting sediments in Keuper facies (K) and the top of a dolerite sill (Dol); (B): «pillow» structures; (C): «ropy» structure enlarged in (D); (E): «ropy» helicitic structure; (F): detail of E.

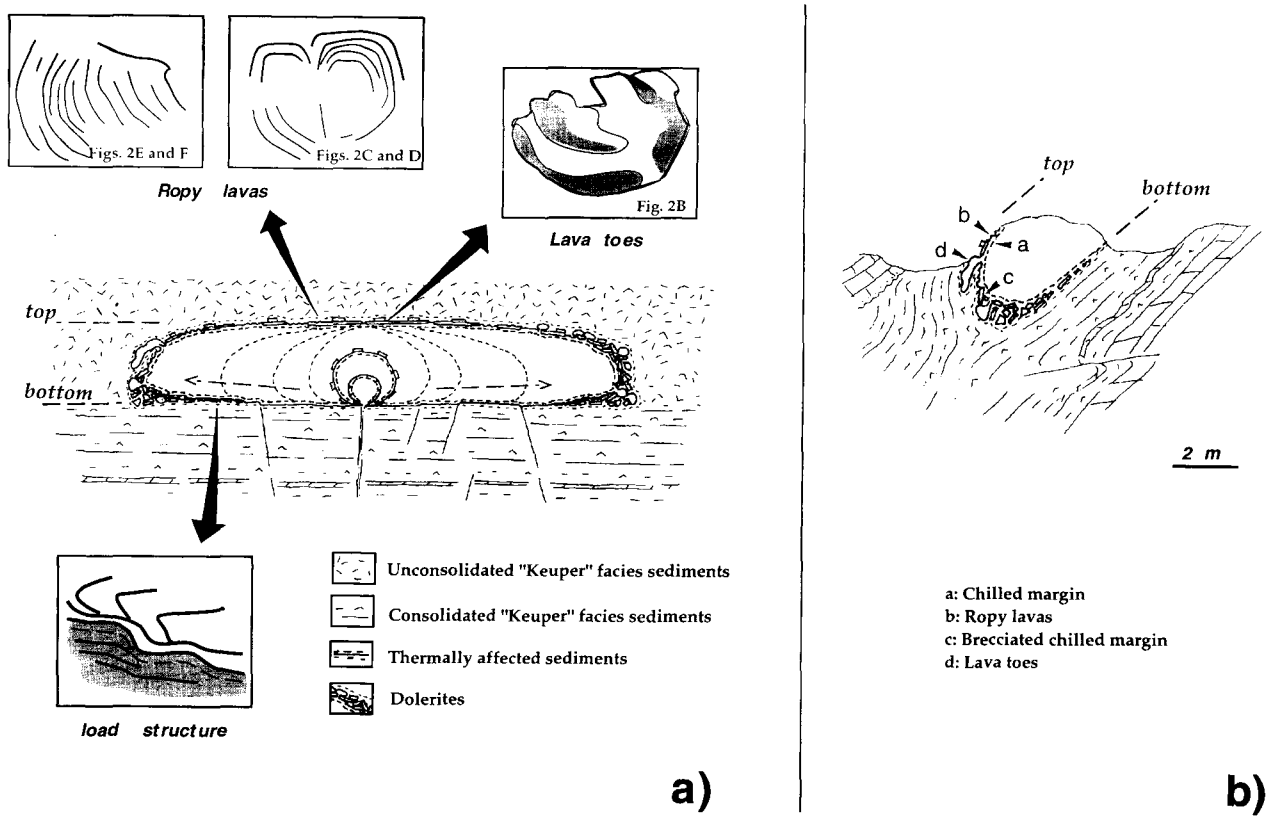

Fig. 3.—(a) Schematic dolerite emplacement model with location of structures shown in Fig. 2. (b) idealized outcrop section, showing the relative location of ropy structures and lava toes.

Mineral	*Chilled and central facies*	*Pegmatitoid fac.*
Ol	(Chl)	
Cpx	$Fs_{3.38}$ — $Fs_{7.35}$ — $Fs_{12.06}$	$Fs_{7.04}$ — $Fs_{12.95}$
Pl	$An_{87.09}$ — $An_{78.51}$ — $An_{62.92}$	$An_{59.16}$ — $An_{50.83}$
Am		mg^*: 0.58-0.17
Bt	mg^*: 0.52-0.47	—
Ilm	—	—
Kfs		—
Qtz		—

Fig. 4.—Cristallization sequence in the chilled margin-central facies and the pegmatitoid differentiate (symbols after Kretz, 1983).

cess, increasing the deformation of cover rocks and, finally, cross-cutting the syn-post orogenic molasses and even the Cinca River terraces. The development of these structures covers the Oligocene to Quaternary time-span.

Both subvolcanic doleritic sills are located between the villages of El Grado and Naval (Huesca, Spain: figs. 1B and 1C); they were emplaced in loosely consolidated evaporitic and marly-clayey sediments in Keuper facies in the core of the diapir,

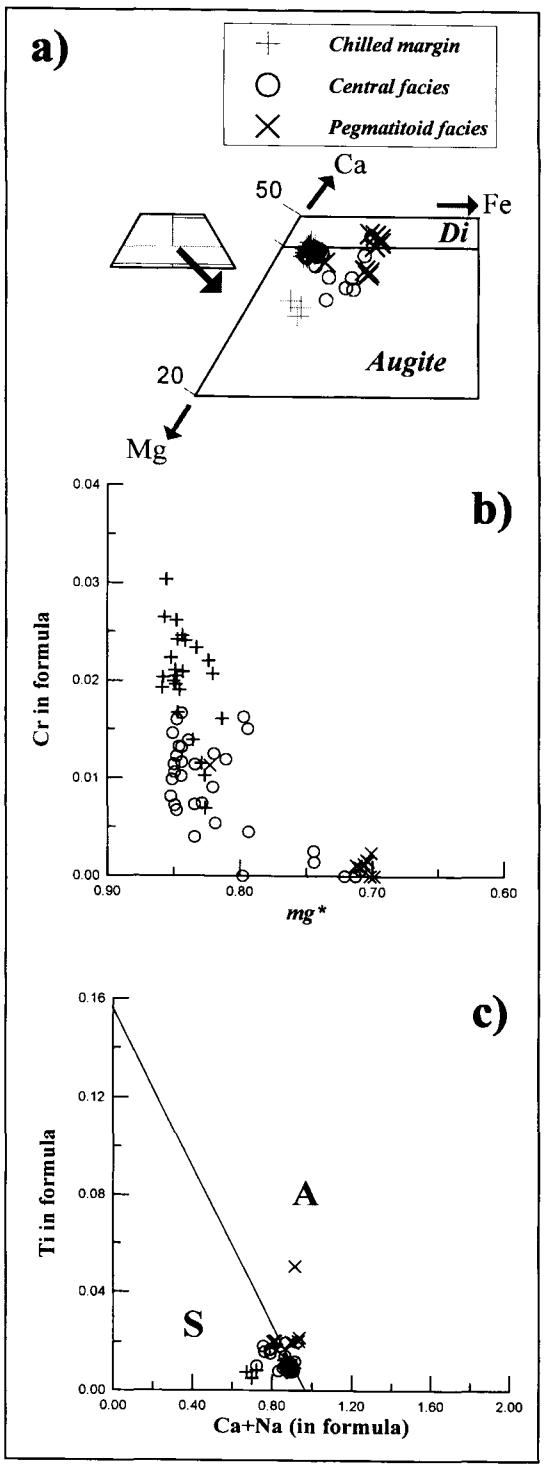

Fig. 5.—Pyroxene composition: a) classification, according to the IMA recommendations (Morimoto *et al.*, 1988). b) Cr *vs* *mg** plot. *mg** stands for the $Mg/(Mg+Fe^{2+})$ ratio (cations per formula unit), c) Ti *vs* Ca+Na plot (Leterrier *et al.*, 1982). Pyroxenes in the marginal and central facies plot into the subalkaline (S) field and only the more evolved compositions of the pegmatitoid fall into the alkaline field (A).

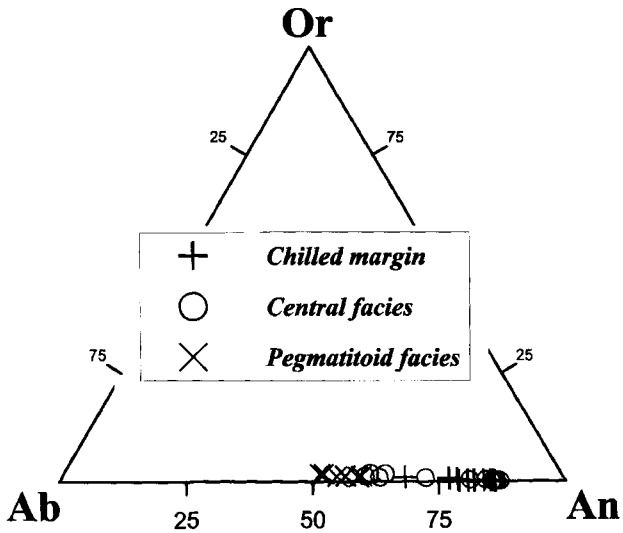

Fig. 6.—Plagioclase classification in the Ab-Or-An system. A progressive variation of the composition is observed from the chilled margin to the central facies and pegmatitoid.

which underwent very low grade contact metamorphism (Lago, 1980). The plasticity of these hosting sediments greatly favoured the magmatic transport and the development of fluidity structures at the top of the sill, and load structures at its base. These processes are the result of the weight of the magmatic mass acting over the hosting materials, under confinement conditions.

Fluidity structures and fragments of the dolerite chilled margin are observed at the top of the sill, under the hosting marly-clayey sediments (fig. 2C and 2E). These fluidity structures show displacement of the magma in different (even opposite) directions within the hosting plastic sediment stratification plane (fig. 2A). Typical examples of fluidity structures are constituted by «pillows» (pillow-sill type, without radial fractures, fig. 2B), flow undulations and «ropy» forms (figs. 2C, 2D, 2E and 2F). Their surfaces are helicoidal (figs. 2C and 2D), and they show multidirectional patterns of magma displacement. Similar structures have been described by Kokelaar (1982 and 1986), Kano (1989) and Morata (1993). These «ropy» structures, similar to those observed in subaerial flows can be explained by the conjunction of three factors: *a)* the low viscosity of the basaltic magma and also *b)* the low viscosity of the hosting plastic sediments, still unconsolidated and water-saturated. These two conditions lead to a low viscosity contrast; finally *c)* the injection of the magma as a wedge, expanding laterally between relatively more competent sedimentary levels.

In a few cases, isolated or coalescent degassing vesicles appear (usually filled with epidote). Load and

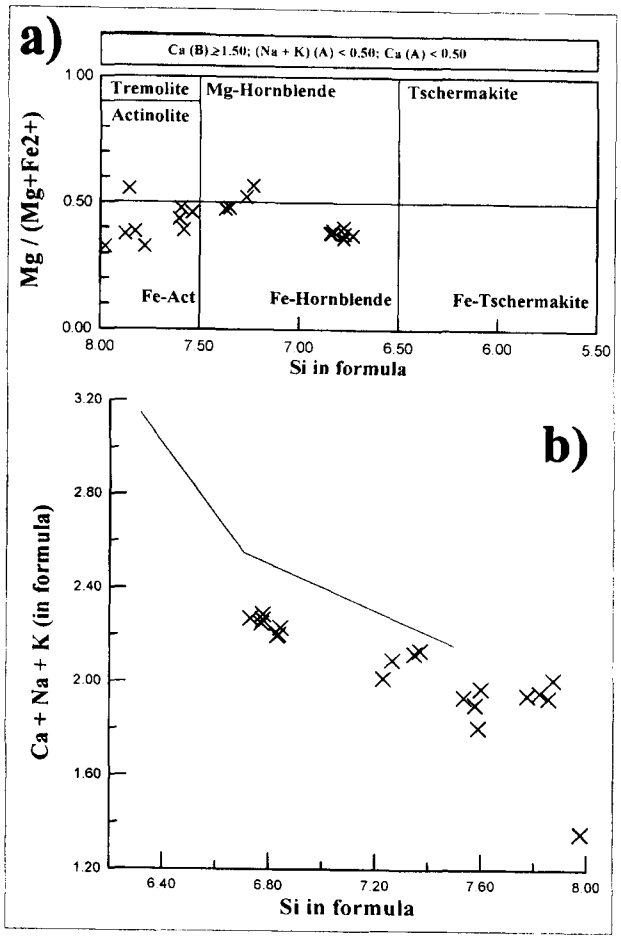

Fig. 7.—Amphibole composition in the pegmatitoid differentiate. a) classification, according to the IMA recommendations (Leake *et al.*, 1997). All the compositions belong to the calcic group. b) CNK *vs* Si diagram. The line represents the limit between the igneous and subsolidus compositions proposed by Leake (1971).

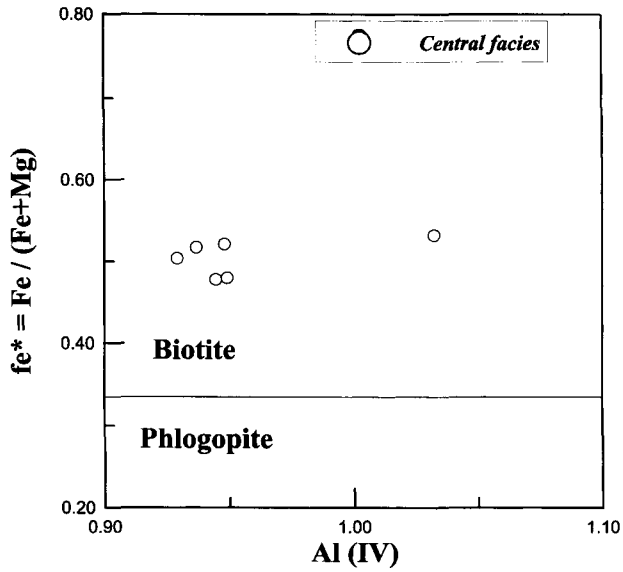

Fig. 8.—Biotite classification, according to Deer *et al.* (1966).

Table 1.—**Chlorite composition (28 Oxygens)**

	1	2
SiO_2	55.711	56.713
TiO_2	0.087	0.000
Al_2O_3	1.363	1.114
FeO(t)	8.824	8.189
MnO	0.108	0.093
MgO	21.428	24.048
CaO	0.891	0.592
Na_2O	0.102	0.049
K_2O	0.103	0.032
Rb_2O	0.084	0.065
BaO	0.000	0.000
F	0.168	0.051
H_2O	13.157	13.588
TOTAL	102.026	104.534
Si	10.102	9.997
Al_{IV}	0.000	0.000
ΣT:	10.102	9.997
Al_{VI}	0.291	0.231
Ti	0.012	0.000
Fe^{3+}	0.000	0.000
Fe^{2+}	1.338	3.622
Mn	0.017	0.014
Mg	5.791	6.318
Ca	0.173	0.112
Na	0.018	0.008
K	0.012	0.004
Rb	0.005	0.004
Ba	0.000	0.000
F	0.004	0.001
ΣY:	7.661	10.314
OH^-	16.000	16.000
TOTAL	33.763	36.311
Classification	Clinochlore	Clinochlore

accomodation structures of the chilled margin to the hosting plastic sediments are common at the base of the sill. These elements, as well as the weak contact metamorphism of the hosting Keuper sediments, and the absence of aerial structures, indicate an emplacement coetaneous or slightly subsequent to the Late Triassic sedimentation. This kind of emplacement into unconsolidated materials (fig. 3A and 3B) excludes the effect of the lithostatic pressure caused by the weight of a significant sedimentary column (Lago & Pocovi, 1982). Thus, emplacement happened before the sedimentation of the Rhaetian and Liassic calcareous series. The range of radiometric ages (187-197±7 Ma) obtained in other Pyrenean dolerites (Montigny *et al.*, 1982, Walgenwitz, 1976 & Beziat, 1983), compared with the new Mesozoic age scale (Gradstein *et al.*, 1994), shows that the dolerite was probably emplaced during the Liassic (between the

Table 2.—**Selected clinopyroxene compositions (1-3: chilled margin; 4-7: central facies and 8-11: pegmatitoid differentiate) (6 O)**

	1	2	3	4	5	6	7	8	9	10	11
SiO_2	49.895	51.448	50.306	51.547	50.16	52.018	50.801	49.198	50.074	50.472	49.645
TiO_2	0.364	0.178	0.339	0.325	0.554	0.36	0.323	1.744	0.683	0.593	0.701
Al_2O_3	2.343	1.487	2.459	2.052	2.261	1.253	2.147	2.097	1.835	3.368	1.919
V_2O_3	0.055	0.036	0.029	0.074	0.095	0.059	0.053	0.156	0.118	0.047	0.131
Cr_2O_3	0.677	0.344	0.663	0.54	0.084	0	0.487	0.054	0.041	0.381	0.05
Fe_2O_3	6.91	5.826	6.05	4.461	5.983	4.021	5.627	4.894	5.65	4.669	5.764
MgO	17.549	20.22	17.924	17.832	17.096	18.865	17.631	13.83	14.347	17.443	15.283
MnO	0.274	0.249	0.096	0.205	0.112	0.277	0.163	0.346	0.373	0.126	0.331
CoO	0.015	0	0	0.026	0.007	0	0	0	0	0	0
NiO	0	0.052	0.065	0	0.02	0.059	0.068	0	0.052	0.182	0
SrO	0	0.033	0	0	0	0	0	0.02	0	0	0
CaO	21.84	16.991	20.847	20.948	18.21	17.709	21.608	21.82	21.246	20.26	19.152
Na_2O	0.166	0.142	0.198	0.205	0.205	0.137	0.161	0.22	0.262	0.133	0.233
K_2O	0.005	0.001	0	0	0.001	0	0	0.016	0.008	0	0
ZnO	0	0.052	0	0.04	0	0	0.014	0	0	0	0
FeO	0	2.839	0.728	2.094	5.586	5.239	0.942	6.359	6.031	2.921	6.803
TOTAL	100.093	99.898	99.704	100.349	100.374	99.997	100.025	100.754	100.72	100.595	100.012
Si	1.91	1.94	1.91	1.93	1.92	1.95	1.92	1.89	1.93	1.89	1.92
Al_{IV}	0.09	0.06	0.09	0.07	0.08	0.05	0.08	0.10	0.07	0.11	0.08
Fe^{3+} (T)	0.00	0.00	0.00	0.00	0.00	0.00	0.00	0.00	0.00	0.00	0.00
Σ T	2.00	2.00	2.00	2.00	2.00	2.00	2.00	1.99	2.00	2.00	2.00
Al_{VI}	0.01	0.01	0.02	0.02	0.02	0.01	0.02	0.00	0.01	0.04	0.01
Fe^{3+} (M1)	0.00	0.00	0.00	0.00	0.00	0.00	0.00	0.00	0.00	0.00	0.00
Ti	0.01	0.01	0.01	0.01	0.02	0.01	0.01	0.05	0.02	0.02	0.02
Cr	0.02	0.01	0.02	0.02	0.00	0.00	0.01	0.00	0.00	0.01	0.00
V	0.00	0.00	0.00	0.00	0.00	0.00	0.00	0.00	0.00	0.00	0.00
Zn	0.00	0.00	0.00	0.00	0.00	0.00	0.00	0.00	0.00	0.00	0.00
Mg (M1)	0.96	0.97	0.95	0.95	0.96	0.98	0.96	0.79	0.82	0.93	0.88
Fe^{2+} (M1)	0.00	0.00	0.00	0.00	0.00	0.00	0.00	0.15	0.14	0.00	0.08
Mn (M1)	0.00	0.00	0.00	0.00	0.00	0.00	0.00	0.00	0.00	0.00	0.00
Σ M1	1.00	1.00	1.00	1.00	1.00	1.00	1.00	1.00	1.00	1.00	1.00
Mg (M2)	0.04	0.17	0.07	0.04	0.02	0.08	0.04	0.00	0.00	0.05	0.00
Fe^{2+} (M2)	0.07	0.14	0.08	0.11	0.24	0.20	0.08	0.10	0.11	0.14	0.20
Mn (M2)	0.01	0.01	0.00	0.01	0.00	0.01	0.01	0.01	0.01	0.00	0.01
Ca	0.89	0.69	0.85	0.84	0.75	0.71	0.88	0.90	0.88	0.81	0.79
Na	0.01	0.01	0.01	0.01	0.02	0.01	0.01	0.02	0.02	0.01	0.02
K	0.00	0.00	0.00	0.00	0.00	0.00	0.00	0.00	0.00	0.00	0.00
Ni	0.00	0.00	0.00	0.00	0.00	0.00	0.00	0.00	0.00	0.01	0.00
Co	0.00	0.00	0.00	0.00	0.00	0.00	0.00	0.00	0.00	0.00	0.00
Sr	0.00	0.00	0.00	0.00	0.00	0.00	0.00	0.00	0.00	0.00	0.00
Σ M2	1.03	1.02	1.02	1.01	1.02	1.01	1.02	1.03	1.02	1.01	1.02
TOTAL	4.03	4.02	4.02	4.01	4.02	4.01	4.02	4.02	4.02	4.01	4.02
*mg**	0.85	0.83	0.85	0.85	0.74	0.80	0.85	0.70	0.71	0.82	0.70
Wo	45.62	34.89	43.64	43.25	38.13	36.15	44.84	46.26	44.98	42.30	40.69
En	51.00	57.76	52.20	51.22	49.80	53.58	50.90	40.79	42.25	50.66	45.17
Fs	3.38	7.35	4.15	5.53	12.06	10.27	4.26	12.95	12.77	7.04	14.15

Hettangian and Toarcian). This implies that the uppermost section of the Keuper facies and the lowermost calcareous series are Early liassic in this south Pyrenean domain, unless the available radiometric ages (which show a broad dispersion of values) require revision and confirmation using other methods.

Established lithotypes

The established lithotypes (chilled margin, central facies and pegmatitoid differentiate) are similar to those described in other Pyrenean tholeiitic dolerites (Lago, 1980; Azambre *et al.*, 1987). A

Table 3.—**Plagioclase composition (1-2: chilled margin; 3-4: central facies and 5-6: pegmatitoid differentiate) (8 O)**

	1	2	3	4	5	6
SiO_2	47.036	49.388	46.752	53.329	54.557	56.479
Al_2O_3	32.329	30.870	32.668	27.880	27.013	26.352
FeO(t)	0.394	0.574	0.593	1.129	0.847	0.648
MgO	0.210	0.252	0.217	0.146	0.101	0.046
CaO	18.138	16.685	18.480	13.520	12.725	10.941
SrO	0.000	0.055	0.000	0.113	0.022	0.053
Na_2O	1.591	2.464	1.483	4.297	4.714	5.658
K_2O	0.032	0.091	0.047	0.162	0.214	0.288
Rb_2O	0.127	0.067	0.084	0.092	0.095	0.081
BaO	0.055	0.000	0.027	0.000	0.000	0.000
Y_2O_3	0.000	0.043	0.021	0.000	0.000	0.000
TOTAL	99.912	100.489	100.372	100.668	100.288	100.546
Si	2.18	2.26	2.16	2.42	2.48	2.54
Al	1.76	1.67	1.78	1.49	1.45	1.40
ΣT	3.94	3.93	3.93	3.92	3.92	3.94
Fe (t)	0.02	0.02	0.02	0.04	0.03	0.02
Mg	0.01	0.02	0.01	0.01	0.01	0.00
Ca	0.90	0.82	0.91	0.66	0.62	0.53
Sr	0.00	0.00	0.00	0.00	0.00	0.00
Na	0.14	0.22	0.13	0.38	0.42	0.49
K	0.00	0.01	0.00	0.01	0.01	0.02
Rb	0.00	0.00	0.00	0.00	0.00	0.00
Ba	0.00	0.00	0.00	0.00	0.00	0.00
Y	0.00	0.00	0.00	0.00	0.00	0.00
TOTAL	5.02	5.02	5.02	5.02	5.01	5.01
Ab:	13.67	20.98	12.65	36.19	39.66	47.57
An:	86.14	78.51	87.09	62.92	59.16	50.83
Or:	0.18	0.51	0.26	0.90	1.18	1.59

Table 4.—**Amphibole compositions obtained for the pegmatitoid differentiate (23 equivalent O)**

	1	2	3	4
SiO_2	50.494	50.764	49.786	48.882
TiO_2	0.113	0.139	0.136	0.110
Al_2O_3	2.303	2.184	2.142	4.429
V_2O_3	0.064	0.000	0.000	0.099
Cr_2O_3	0.000	0.028	0.027	0.060
FeO(t)	21.818	25.484	24.993	19.741
MgO	10.918	8.906	8.734	11.017
MnO	0.721	0.497	0.487	0.294
NiO	0.000	0.000	0.000	0.016
CaO	10.373	11.441	11.221	12.491
Na_2O	0.874	0.376	0.369	0.501
K_2O	0.064	0.183	0.179	0.344
BaO	0.000	0.000	0.000	0.000
P_2O_5	0.000	0.000	0.000	0.000
H_2O	1.987	0.000	2.000	1.999
F	0.000	0.000	0.000	0.000
TOTAL	99.729	100.002	100.074	99.983
Si	7.59	7.58	7.58	7.27
Al_{IV}	0.41	0.38	0.38	0.73
Ti_T	0.00	0.02	0.02	0.00
Cr_T	0.00	0.00	0.00	0.00
$Fe^{3+}{}_T$	0.00	0.02	0.02	0.00
ΣT	8.00	8.00	8.00	8.00
Al_{VI}	0.00	0.00	0.00	0.04
Ti	0.01	0.00	0.00	0.01
Cr	0.00	0.00	0.00	0.01
Fe^{3+}	0.08	0.08	0.08	0.22
Mg_C	2.45	1.98	1.98	2.44
$Fe^{2+}{}_C$	2.46	2.94	2.94	2.23
Mn_C	0.00	0.00	0.00	0.04
Ni_C	0.00	0.00	0.00	0.00
V_C	0.00	0.00	0.00	0.01
Sc	5.00	5.00	5.00	5.00
Mg_B	0.00	0.00	0.00	0.00
$Fe^{2+}{}_B$	0.20	0.15	0.15	0.00
Mn_B	0.09	0.06	0.06	0.00
Ni_C	0.00	0.00	0.00	0.00
V_C	0.01	0.00	0.00	0.01
Ca	1.67	1.83	1.83	1.99
Na_B	0.02	0.00	0.00	0.00
ΣB	2.00	2.04	2.04	2.00
Na_A	0.11	0.05	0.05	0.07
K	0.01	0.02	0.02	0.03
Ba	0.00	0.00	0.00	0.00
P	0.00	0.00	0.00	0.00
ΣA	0.11	0.07	0.07	0.10
TOTAL	15.11	15.11	15.11	15.11
Group Classification	Calcic Fe-Act	Calcic Fe-Act	Calcic Fe-Act	Calcic Mg-Hbl

centimetric-scale progressive petrographic transition might be observed from the chilled margin towards the inside of the sill, with the following sequence of textures: microdiabasic porphyritic (with skeletal plagioclase crystals), porphyritic subophitic, subophitic and finally, ophitic, which is the main textural typ. The *chilled margin* mineral association consists of olivine (altered to clinochlore-type smectitic and chloritic compositions), augite, plagioclase, and opaque minerals (fig. 4). The *central facies* (95% of the volume) with ophitic or, locally, doleritic ophitic textures, consists of altered olivine (often included in augite), plagioclase, minor amphibole (ferro-hornblende in composition), scarce biotite, chlorite (late phase) and opaque minerals. Small potassic feldspar crystals are present in some cases, usually infilling the mesostasis. The *pegmatitoid differentiate* consists of a centimetric vein of irregular geometry, cross-cutting the other lithotypes. It has a doleritic texture, with major augite and plagioclase development, and with amphibole, biotite, ilmenite, potassic feldspar and quartz filling the intercrystalline spaces (sometimes with micrographic textures; fig. 4).

Table 5.—**Biotite compositions in central facies (22 equivalent O)**

	1	2	3	4	5	6
SiO_2	39.753	38.383	40.340	39.845	37.469	39.231
TiO_2	1.692	1.711	2.034	1.835	1.241	2.062
Al_2O_3	10.605	10.419	10.795	10.439	11.292	10.463
FeO	21.000	23.253	21.671	22.351	23.947	22.977
MnO	0.075	0.048	0.117	0.031	0.021	0.007
MgO	12.798	12.022	13.310	12.376	11.768	12.058
CaO	0.024	0.002	0.126	0.072	0.017	0.048
Na_2O	0.141	0.098	0.096	0.155	0.157	0.143
K_2O	8.637	8.543	8.296	8.769	9.026	8.839
BaO	0.084	0.281	0.165	0.114	0.000	0.060
Rb_2O	0.000	0.000	0.000	0.000	0.000	0.000
H_2O	3.785	3.694	3.869	3.763	3.759	3.744
F	0.251	0.304	0.260	0.338	0.136	0.331
TOTAL	98.845	98.758	101.079	100.088	98.833	99.963
Si	3.049	2.993	3.025	3.039	2.936	3.010
Al_{IV}	0.949	0.948	0.945	0.929	1.032	0.937
$Fe^{3+}{}_T$	0.000	0.000	0.000	0.000	0.008	0.000
Ti_T	0.002	0.059	0.030	0.032	0.024	0.054
ΣZ	4.000	4.000	4.000	4.000	4.000	4.000
Al_{VI}	0.000	0.000	0.000	0.000	0.000	0.000
Fe^{3+}	0.000	0.000	0.000	0.000	0.000	0.000
Ti	0.096	0.041	0.084	0.074	0.049	0.065
Mg	1.463	1.397	1.488	1.407	1.374	1.379
Fe^{2+}	1.349	1.520	1.362	1.429	1.562	1.477
Mn	0.005	0.003	0.007	0.002	0.001	0.000
ΣY	2.913	2.962	2.941	2.911	2.987	2.922
K	0.845	0.850	0.794	0.853	0.902	0.865
Na	0.021	0.015	0.014	0.023	0.024	0.021
Ca	0.002	0.000	0.010	0.006	0.001	0.004
Rb	0.000	0.000	0.000	0.000	0.000	0.000
Ba	0.003	0.009	0.005	0.003	0.000	0.002
ΣX	0.871	0.873	0.823	0.885	0.927	0.892
F	0.061	0.075	0.062	0.082	0.034	0.080
OH	1.937	1.921	1.935	1.915	1.965	1.916
ΣA	1.997	1.996	1.997	1.996	1.998	1.996
TOTAL	7.784	7.836	7.764	7.797	7.914	7.814
mg*	47.976	52.106	47.790	50.387	53.197	51.723

Mineral composition

Mineral composition was obtained with CAMECA SX-50 microprobes (Barcelona, Toulouse and Oviedo universities) under standard conditions (15Kv, 10nA, 1 mm beam diameter and 10 seconds integration time). Except for the olivine (altered to clinochlore: table 1), the centre-to-edge profiles reflect the complete evolution of mineral phases.

Clinopyroxene: augite and diopside (table 2), displaying and increase in Fe (and Na), from the chilled margin to the centre and, finally, to the pegmatitoid (fig. 5a). This trend becomes more obvious in a Cr *vs mg** plot (fig. 5b), where a differentiation — decrease in Cr— at nearly constant mg* values can be observed from the chilled margin to the central facies. Only the pyroxenes in the pegmatitoid show a marked decrease in mg*, with very low Cr values. The low Ti content (with higher values for the pegmatitoid: table 2) and (Ca+Na) values indicate the subalkaline composition of the rocks (fig. 5c; Leterrier *et al.*, 1982). The absence of pigeonite (usually typical of these rocks) (Lago, 1980; Azambre *et al.*, 1987) can be explained in relation with a more fractioned liquid with relatively high fO_2 values.

Plagioclase: Together with pyroxene, it constitutes the major mineral phase in the rock (40-52%). It has a characteristic zonation, low K content, and its composition ranges in the An_{86-50} interval (table 3), with decreasing values as crystallization progresses (fig. 6). It reaches a compositional minimum (An_{59-50}) in the pegmatitoid differentiate.

Amphibole and biotite: The presence of large amphibole crystals is typical of the pegmatitoid (5-6 %), showing Fe-rich compositions both in initial (Fe-hornblende) and in late compositions (Fe-actinolite and Fe-hornblende) —fig. 7A— (IMA, 1997) and table 4. Its composition (without Al^{VI} and Ti: table 4), as represented in the CNK *vs* Si system (fig. 7B; Leake, 1971) is consistent with a gradual evolution from igneous Fe-hornblendes (Si < 7.5), to Fe-actinolites (Si > 7.5), characteristic of late crystallization under subsolidus conditions. This means that amphibole crystallizes in successively silicon-richer and ferrous conditions, and under Na- and Al- depleted conditions (table 4). This can be explained by the inclusion of these elements in the later, more sodic, plagioclase.

Biotite is a minor phase (< 1 %) in the central facies, but is more abundant in the pegmatitoid differentiate (1-2 %). We only analyzed crystals of the central facies and their compositions (table 5), present and almost constant *fe** value (fig. 8: *fe** stands for the $Fe^{2+}/(Fe^{2+} + Mg)$ ratio).

Accessory minerals: opaque minerals in the chilled margin and the central facies are scarce (< 1 %) and altered, but they are abundant in the pegmatitoid differentiate (2 %). They are ususally ilmenite or magnetite (table 6). These ilmenites crystallized later; they have microscopic rutile inclusions and their edges are leucoxene or pseudo-brookite. These microtextural criteria indicate that ilmenite may have undergone late destabilization processes, thus precluding the use of geothermometers. Sulfides are scarce (< 1 %), and mostly pyrite (table 7). Common feldspar-quartz and albite-quartz intergrowths constitute late-crystallization minerals (Lago, 1980; Azambre *et al.*, 1987).

The most frequent secondary minerals (< 0.2 % in central facies and < 1 % in the pegmatitoid) are chlorite (clinochlore; table 1) which replaces olivine, and epidote (pistacite; table 8), which is more

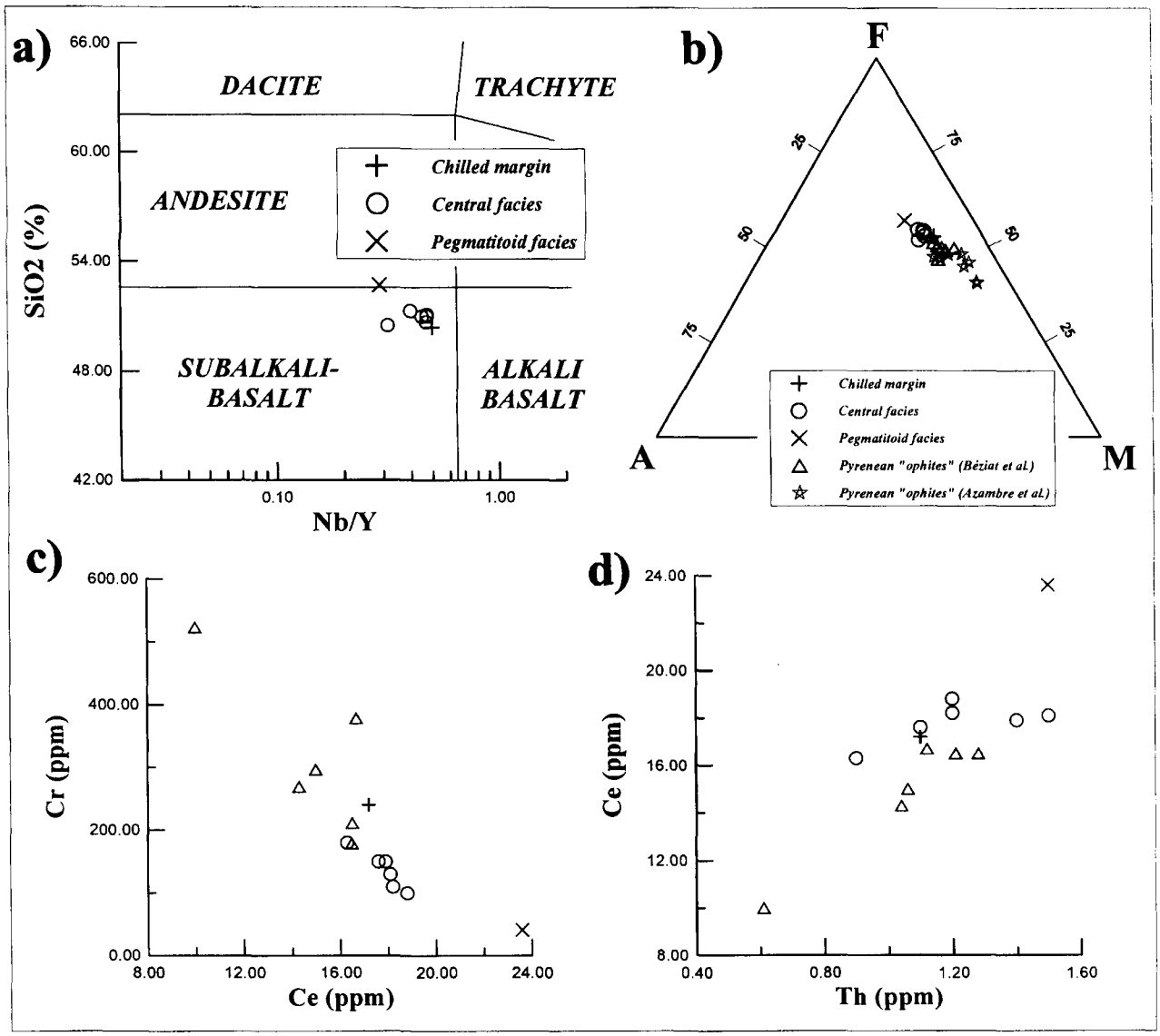

Fig. 9.—a) Rock classification in the $\%SiO_2$ *vs* Nb/Y system (Winchester & Floyd, 1973). b) AFM diagram, showing the compositions of the studied rocks and, also, composition of the less evolved «ophites» analysed by Beziat *et al.* (1991) and Azambre *et al.* (1987). Note the increase of the F/M ratio, typical of tholeiitic series. c) Cr *vs* Ce plot and d) Ce *vs* Th plot show nearly linear differentiation trends, typical of a fractional crystallization process.

abundant in the pegmatitoid. Prehnite appears occasionally in these rocks.

Geochemical composition

Table 9 shows 8 new analyses of unaltered rocks (average L.O.I. in 1.18 %) analyzed by FRX and ICP-MS at the XRAL Laboratory (Toronto, Canada), together with the average of 6 other south Pyrenean «ophites» (Beziat *et al.*, 1991). Their subalkaline composition might be deduced from the $\%SiO_2$ *vs* Nb/Y diagram (fig. 9a; Winchester & Floyd, 1973). The *mg** (Mg/Mg+Fe) range of 0.61-0.53, together with the Ni (86-43 ppm) and Cr ranges (240-41 ppm) suggest differentiated liquids with chilled margin fractionation in relation to the central facies. This is even more clear in the pegmatitoid. Fractionation (AFM in fig. 9b) is also shown by the relations between the compatible (e.g. Cr; fig. 9c) and incompatible (e.g. Ce, Th; fig. 9d) elements. These fractionation trends are mainly controlled by the pyroxene modal proportion and evolution (Cr and Co). The rare olivine

Table 6.—**Ilmenite composition (1-3: central facies and 4-8: pegmatitoid differentiate) (6 O)**

	1	2	3	4	5	6	7	8
TiO_2	53.315	52.978	51.718	51.536	49.939	49.669	49.917	49.377
SiO_2	0.172	0.054	0.027	0.290	0.057	0.020	0.035	0.309
FeO	42.204	46.160	35.924	34.109	36.397	35.432	35.236	34.977
Cr_2O_3	0.068	0.052	0.305	0.171	0.066	0.000	0.000	0.048
Al_2O_3	0.060	0.076	0.693	0.708	0.077	0.099	0.058	0.040
V_2O_3	1.729	1.703	1.575	1.545	0.000	0.000	0.000	0.000
MnO	5.500	0.945	11.016	12.052	8.463	9.144	9.499	9.304
MgO	0.136	0.336	0.032	0.341	0.013	0.022	0.040	0.029
CaO	0.436	0.124	0.098	0.108	0.000	0.000	0.000	0.000
TOTAL	103.620	102.428	101.388	100.860	95.011	94.387	94.784	94.085
Ti	1.95	1.96	1.93	1.93	1.99	2.00	2.00	1.99
Si	0.01	0.00	0.00	0.01	0.00	0.00	0.00	0.02
Fe^{3+}	0.00	0.00	0.00	0.00	0.00	0.00	0.00	0.00
Cr	0.00	0.00	0.01	0.01	0.00	0.00	0.00	0.00
Al	0.00	0.00	0.04	0.04	0.00	0.01	0.00	0.00
V	0.07	0.07	0.06	0.06	0.00	0.00	0.00	0.00
Fe^{2+}	1.72	1.90	1.49	1.42	1.62	1.58	1.57	1.56
Mn	0.23	0.04	0.46	0.51	0.38	0.41	0.43	0.42
Mg	0.01	0.02	0.00	0.03	0.00	0.00	0.00	0.00
Ca	0.02	0.00	0.00	0.00	0.00	0.00	0.00	0.00
TOTAL	4.00	4.00	4.01	4.00	4.00	4.00	4.00	4.00

Table 7.—**Sulphide composition in the pegmatitoid facies**

	1	2
S	67.345	66.776
Fe	32.310	32.833
Cu	0.000	0.017
As	0.045	0.000
Co	0.091	0.064
Zn	0.000	0.000
Pb	0.000	0.000
Bi	0.034	0.000
Sb	0.013	0.032
Ni	0.120	0.211
Au	0.000	0.000
Ag	0.000	0.026
Te	0.000	0.000
Se	0.000	0.000
Cd	0.014	0.041
Sn	0.028	0.000
TOTAL	100.000	100.000

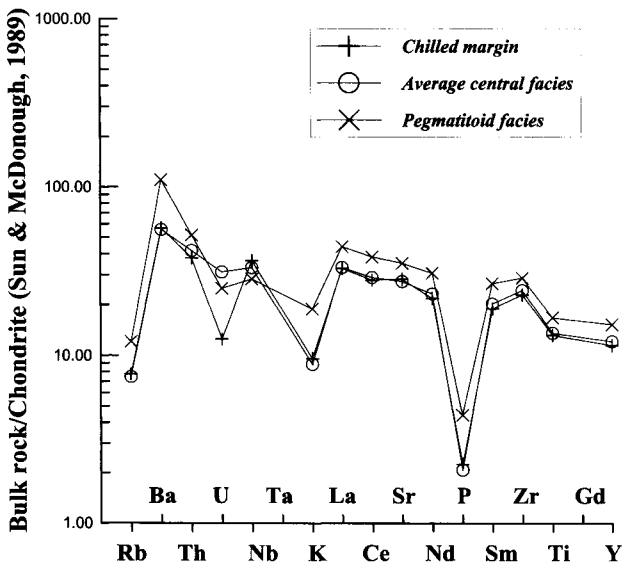

Fig. 10.—Chondrite-normalized multielement —*spider*— plot. Note the coincidence of the chilled margin and central facies patterns.

(with a high partition coefficient for Ni) has almost no significance in our rocks, in contrast to other south Pyrenean ophites with higher proportions of this mineral (Azambre *et al.*, 1987; Beziat *et al.*, 1991). Plagioclase fractionation has been confirmed by the increase in Eu, with higher values for the pegmatitoid. These patterns indicate a slightly higher differentiation in our rocks (from the southern Pyrenees) in relation to other ophites located closer to the central Pyrenees (Beziat *et al.*, 1991). Ti (0.98 % in the chilled margins) presents higher values in the pegmatitoid (1.24 %) where late ilmenite concentrates. Amphibole and biotite contents show a relative enrichment in Ti, Zr and Nb, which becomes more evident in the REE analysis (Ce, Nd, Gd, Dy and Er).

Table 8.—**Epidote (pistacite) composition in the pegmatitoid differentiate (12,5 O).**

	1	2	3	4	5	6	7	8
SiO_2	37.978	37.357	37.759	37.428	38.140	37.634	38.507	37.462
TiO_2	0.053	0.049	0.129	0.082	0.100	0.989	0.162	0.027
Al_2O_3	22.731	21.186	21.625	21.131	23.263	21.766	22.761	24.816
Cr_2O_3	0.000	0.054	0.000	0.000	0.000	0.002	0.000	0.000
Y_2O_3	0.062	0.037	0.000	0.000	0.050	0.037	0.000	0.000
FeO	12.716	14.772	14.059	14.388	11.229	12.576	12.700	10.236
MnO	0.040	0.152	0.194	0.098	0.089	0.252	0.326	0.220
MgO	0.041	0.000	0.007	0.007	0.000	0.009	0.000	0.000
CaO	24.690	24.514	24.330	24.522	24.623	24.239	24.376	24.757
SrO	0.570	0.342	0.351	0.380	0.065	0.547	0.332	0.408
Na_2O	0.002	0.014	0.011	0.000	0.037	0.020	0.003	0.000
K_2O	0.014	0.002	0.005	0.000	0.000	0.000	0.000	0.000
P_2O_5	0.071	0.048	0.057	0.000	0.075	0.040	0.066	0.662
H_2O	1.846	1.816	1.826	1.810	1.843	1.828	1.857	1.868
TOTAL	100.814	100.343	100.353	99.846	99.514	99.939	101.090	100.456
Si	3.08	3.08	3.10	3.10	3.10	3.09	3.11	3.01
Al_{IV}	0.00	0.00	0.00	0.00	0.00	0.00	0.00	0.00
ΣT	3.08	3.08	3.10	3.10	3.10	3.09	3.11	3.01
Al_{VI}	2.18	2.06	2.09	2.06	2.23	2.10	2.17	2.35
Fe^{3+}	0.00	0.00	0.00	0.00	0.00	0.00	0.00	0.00
Ti	0.00	0.00	0.01	0.01	0.01	0.06	0.01	0.00
Cr	0.00	0.00	0.00	0.00	0.00	0.00	0.00	0.00
ΣM	2.18	2.07	2.10	2.07	2.24	2.17	2.18	2.35
Fe^{2+}	0.86	1.02	0.97	1.00	0.76	0.86	0.86	0.69
Mg	0.00	0.00	0.00	0.00	0.00	0.00	0.00	0.00
Mn	0.00	0.01	0.01	0.01	0.01	0.02	0.02	0.01
Y	0.00	0.00	0.00	0.00	0.00	0.00	0.00	0.00
Ca	2.15	2.17	2.14	2.18	2.15	2.13	2.11	2.13
Sr	0.03	0.02	0.02	0.02	0.00	0.03	0.02	0.02
Na	0.00	0.00	0.00	0.00	0.01	0.00	0.00	0.00
K	0.00	0.00	0.00	0.00	0.00	0.00	0.00	0.00
P	0.00	0.00	0.00	0.00	0.01	0.00	0.00	0.04
ΣX	3.06	3.22	3.14	3.20	2.93	3.04	3.01	2.89
TOTAL	10.16	10.19	10.17	10.17	10.11	10.12	10.15	10.12

The multielemental pattern normalized to chondrite (Sun & McDonough, 1989) shows (fig. 10) high Ba and Th contents, a strong negative anomaly in P, low Ti values, and slightly decreasing values of La-Nd and Zr-Y. The REE pattern (fig. 11), normalized to MORB-N (Hoffmann, 1988) shows a slight enrichment in LREE and a depletion in HREE, together with a weak positive Eu anomaly. Both diagrams evidence a weak fractionation of the chilled margin and central facies, a process which is slightly stronger in the pegmatitoid. On the other hand, the scarce data from other south Pyrenean «ophites» (fig. 11; values from Beziat *et al.*, 1991) fit the observed pattern.

A tholeiitic affinity can be deduced by the average ratios (table 10) of Nb/Y, Th/La, Th/Hf, La/Lu, La/Yb and K/Rb, together with low TiO_2 and P_2O_5 values, which are consistent with the ratios of Zr/TiO_2, Ti/Zr, Ti/V, Nb/Zr and Y/Zr relations (table 10). Additionally, the alkalinity index (A.I. = $Na_2O + K_2O/(SiO_2\text{-}43) \times 0.17$; Middlemost, 1975) values, with an 1.99 average also indicate this tholeiitic affinity, when plotted against Al_2O_3 (fig. 12A). The obtained values coincide well with those from other Pyrenean continental tholeiites ——«ophites»— (Alibert, 1985; Beziat *et al.*, 1991). However, the mineral associations of our rocks show, a higher degree of differentiation than other samples from the internal Pyrenees, where occasional olivine cumulates or slight enrichments in this mineral might be observed (Azambre *et al.*, 1987). This pattern of higher differentiation can be deduced in the Cr *vs mg** (fig. 12B) diagram, where the values of Azambre *et al.* (1987) and Beziat *et al.* (1991) have also been plotted. This behaviour suggests an evolution of these tholeiitic liquids from the centre (first stage) towards the external zones of the Pyrenees (late stages).

Table 9.—**Whole rock chemical composition (anal.1: chilled margin; 2-7: central facies; 8: pegmatitoid differentiate, and column 9: average of analyses of Beziat *et al.*, 1991).**

	1	2	3	4	5	6	7	8	9
SiO_2	50.40	51.00	51.30	50.70	51.00	50.50	51.10	52.70	50.933
TiO_2	0.98	1.06	1.07	0.93	1.03	0.99	0.95	1.24	1.006
Al_2O_3	14.20	15.10	15.10	15.60	15.10	14.70	14.80	13.30	15.067
Fe_2O_3	11.10	11.00	11.20	10.30	11.00	11.10	10.70	12.00	10.833
MnO	0.18	0.19	0.18	0.17	0.17	0.18	0.18	0.19	0.178
MgO	7.62	7.09	6.92	6.66	6.43	6.76	6.65	5.83	6.752
CaO	11.40	9.82	10.90	11.70	11.20	11.20	11.20	9.44	11.003
Na_2O	1.66	2.19	1.90	2.09	2.26	2.09	2.08	2.00	2.102
K_2O	0.63	0.94	0.67	0.42	0.50	0.48	0.49	1.24	0.583
P_2O_5	0.11	0.12	0.12	0.11	0.12	0.12	0.11	0.15	0.117
L.O.I.	1.00	1.65	0.80	1.05	1.10	1.10	1.10	1.65	1.133
*mg**	0.61	0.59	0.58	0.60	0.57	0.58	0.59	0.53	0.586
TOTAL	99.26	100.16	100.16	99.73	99.91	99.22	99.36	99.74	99.757
Cl	929.00	941.00	1470.00	888.00	641.00	605.00	645.00	2.190.00	865.000
Li	15.00	14.00	15.00	5.00	6.00	6.00	6.00	36.00	8.667
B	30.00	44.00	38.00	22.00	39.00	16.00	12.00	36.00	28.500
S	260.00	350.00	330.00	240.00	290.00	290.00	230.00	90.00	288.333
Sc	38.00	38.00	38.00	36.00	38.00	38.00	38.00	41.00	37.667
V	210.00	196.00	245.00	236.00	238.00	197.00	253.00	328.00	227.500
Cr	240.00	110.00	100.00	180.00	130.00	150.00	150.00	41.00	136.667
Co	39.00	35.00	35.00	35.00	35.00	36.00	35.00	28.00	35.167
Ni	86.00	52.00	48.00	57.00	53.00	57.00	59.00	43.00	54.333
Cu	122.00	135.00	135.00	113.00	123.00	129.00	125.00	115.00	126.667
Zn	84.10	116.00	152.00	57.70	50.10	56.30	60.60	52.10	82.117
Rb	18.00	29.00	20.00	13.00	12.00	15.00	15.00	28.00	17.333
Sr	207.00	237.00	187.00	189.00	206.00	193.00	189.00	257.00	200.167
Y	18.00	20.00	20.00	17.00	19.00	19.00	19.00	24.00	19.000
Zr	89.00	101.00	97.00	87.00	94.00	94.00	93.00	112.00	94.333
Nb	9.00	9.00	8.00	8.00	9.00	6.00	9.00	7.00	8.167
Ba	137.00	97.00	197.00	90.00	136.00	156.00	131.00	266.00	134.500
La	7.80	8.10	8.40	7.10	8.10	8.00	7.80	10.50	7.917
Ce	17.20	18.20	18.80	16.30	18.10	17.90	17.60	23.60	17.817
Pr	2.30	2.40	2.50	2.20	2.50	2.40	2.40	3.30	2.400
Nd	10.20	11.10	11.40	10.00	11.10	10.80	10.70	14.40	10.850
Sm	2.90	3.20	3.20	2.80	3.20	3.20	3.00	4.10	3.100
Eu	1.03	1.09	1.15	1.00	1.11	1.12	1.05	1.46	1.087
Gd	3.20	3.30	3.60	3.00	3.50	3.40	3.20	4.70	3.333
Tb	0.50	0.60	0.60	0.50	0.60	0.60	0.50	0.80	0.567
Dy	3.30	3.60	3.60	3.20	3.60	3.60	3.40	4.70	3.500
Ho	0.67	0.74	0.72	0.63	0.74	0.71	0.68	0.94	0.703
Er	1.90	2.10	2.00	1.80	2.10	2.00	1.90	2.60	1.983
Tm	0.30	0.30	0.30	0.20	0.30	0.30	0.30	0.30	0.283
Yb	1.70	1.90	1.90	1.60	1.90	1.90	1.80	2.10	1.833
Lu	0.25	0.29	0.28	0.24	0.29	0.28	0.27	0.30	0.275
Hf	1.90	2.30	2.30	2.10	2.00	2.10	1.90	2.80	2.117
Ta	0.80	MLD	MLD	0.60	MLD	MLD	0.90	MLD	0.250
Th	1.10	1.20	1.20	0.90	1.50	1.40	1.10	1.50	1.217
U	0.10	0.10	0.40	0.30	0.40	0.30	MLD	0.20	0.250

Conclusions

The El Grado tholeiitic dolerites were emplaced as subvolcanic sills beneath a poorly compacted sheet of marly-evaporitic Keuper sediments. Development of fluidity structures and a very low grade contact metamorphism at the top of the sills indicate that the dolerites where emplaced after the deposition of these sediments and before the Liassic carbonates, concordant with the available radiometric ages. The dolerites

Table 10.—**Interelement ratios and CIPW norm (anal.1: chilled margin; 2-7: central facies; 8: pegmatitoid differentiate; 9: average of analyses of Beziat *et al.*, 1991)**

	1	2	3	4	5	6	7	8	9
Nb/Y	0.500	0.450	0.400	0.471	0.474	0.316	0.474	0.292	0.430
Th/La	0.141	0.148	0.143	0.127	0.185	0.175	0.141	0.143	0.154
Th/Hf	0.579	0.522	0.522	0.429	0.750	0.667	0.579	0.536	0.575
La/Lu	31.200	27.931	30.000	29.583	27.931	28.571	28.889	35.000	28.788
La/Yb	4.588	4.263	4.421	4.438	4.263	4.211	4.333	5.000	4.318
K/Rb	290.570	269.099	278.117	268.218	345.917	265.664	271.199	367.660	279.394
Zr/TiO_2	91.282	95.283	90.654	93.649	91.262	94.758	97.587	90.323	93.802
Ti/Zr	65.665	62.907	66.119	64.005	65.679	63.256	61.422	66.362	63.901
Ti/V	27.829	32.417	26.178	23.595	25.940	30.183	22.578	22.660	26.497
Nb/Zr	0.101	0.089	0.082	0.092	0.096	0.064	0.097	0.063	0.087
Y/Zr	0.202	0.198	0.206	0.195	0.202	0.202	0.204	0.214	0.201
CIPW Norm									
Q	8.560	7.570	9.230	7.730	8.140	8.270	8.980	12.620	8.320
Or	3.720	5.560	3.960	2.480	2.950	2.840	2.900	7.330	3.450
Ab	14.050	18.530	16.080	17.690	19.120	17.690	17.600	16.920	17.790
An	29.440	28.600	30.900	31.950	29.580	29.310	29.600	23.650	29.960
Di	18.450	12.760	15.240	17.760	17.340	17.690	17.630	14.500	16.400
Hy	10.420	11.740	10.170	8.350	7.970	8.630	8.390	7.800	9.210
Il	0.390	0.410	0.390	0.360	0.360	0.390	0.390	0.410	0.380
Hem	11.100	11.000	11.200	10.300	11.000	11.100	10.700	12.000	10.830
Ti	1.910	2.080	2.130	1.810	2.060	1.930	1.830	2.520	1.980
Ap	0.250	0.280	0.280	0.250	0.280	0.280	0.250	0.350	0.270

[1] The term pegmatitoid is used in this paper in the strict sense proposed by Lacroix (1928) in Tomkeieff (1983): «A coarse-grained differentiate of basaltic rocks occurring as dykes, veins or streaks.»

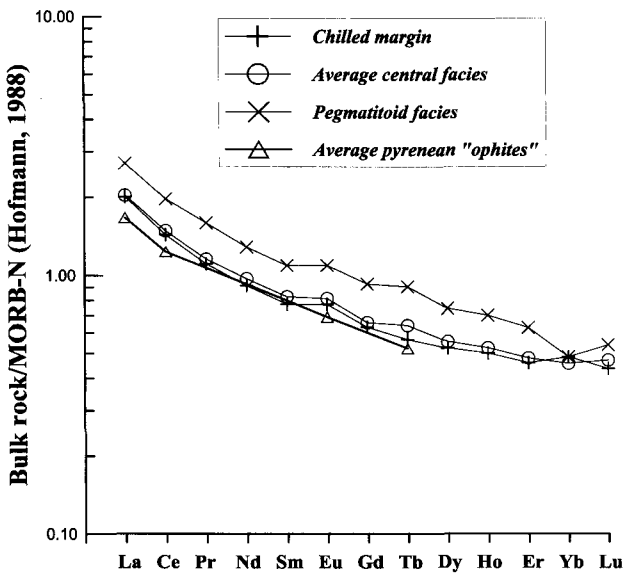

Fig. 11.—REE patterns, normalized to MORB-N (Hoffmann, 1988). Only the pegmatitoid facies displays a significant fractionation.

show a progressive transition from the chilled margin (olivine + augite + plagioclase) towards the central facies (rare olivine + augite + plagioclase + amphibole + biotite). The later is cross-cutted by rare and highly differentiated pegmatitoid veins (Fe-rich augite + Na-rich plagioclase + Fe-rich amphibole + biotite + feldspar + quartz + ilmenite). The compositional study of the major (augite and plagioclase) and late (amphibole and biotite) mineral phases allows us to suggest a mechanism of compositional crystallization evolution from the initial towards the final stages. The geochemical analysis (major, trace and REE elements) reveals a tholeiitic composition with a marked fractionation between the three established lithotypes. The compositional range of these south-Pyrenean tholeiites involves more fractionated liquids than other similar tholeiites of the central Pyrenees.

ACKNOWLEDGEMENTS

The authors would like to thank Drs. J. López Ruiz and M. Doblas (MNCN, CSIC, Madrid) for her comments and corrections to previous versions of the manuscript, which have greatly improved the final text.

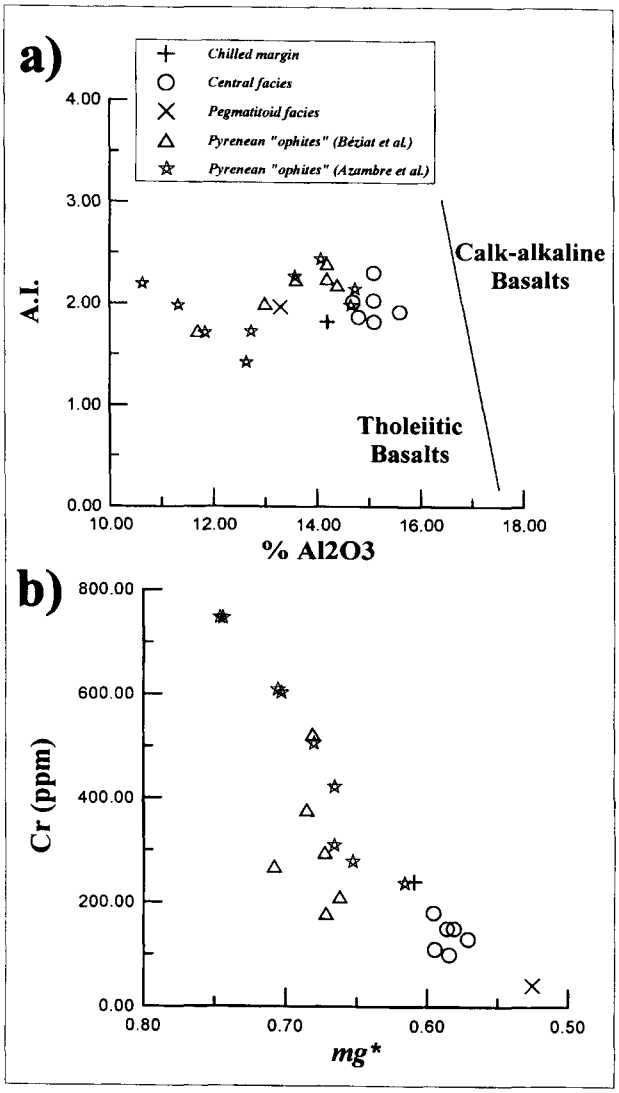

Fig. 12.—a) A.I. *vs* $\%Al_2O_3$ plot, according to Middlemost (1975). b) Cr *vs* *mg** plot for the ophitic rocks considered in this paper.

References

Alibert, C. (1985). A. Sr-Nd isotopic and REE study of late Triassic dolerites from the Pyrenees (France) and the Messejana Dyke (Spain and Portugal). *Earth Planet. Sci. Lett.*, 73, 81-90.

Azambre, B., Rossy, M., and Lago, M. (1987). Caractéristiques pétrologiques des dolérites tholéiitiques d'âge triasique (ophites) du domaine pyrénéen. *Bull. Minéral.*, 110, 379-396.

Bèziat, D. (1983). Etude pétrologique et géochimique des ophites des Pyrénées. Implications géodynamiques. *Thèse 3.e cycle*, Université de Toulouse, 60 pages.

Bèziat, D., Joron, J. L., Monchoux, P., Treuil, M., and Walgenwitz, F. (1991). Geodynamic implications of geochemical data for the Pyrenean ophites (Spain-France). *Chemical Geol.*, 89, 243-262.

Camara, P., and Klimowitz, J. (1985). Interpretación geodinámica de la vertiente centro-occidental surpirenaica. *Estudios Geol.*, 41, 391-404.

Deer, W. A., Howie, R. A., and Zussman, J. (1966). *An introduction to the Rock-forming minerals*. 1.st Ed., 528 pp., Longman.

Gradstein, F. M., Agterberg, F. P., Ogg, J. G., Hardenbol, J., Van Veen, P., Thierry, J., and Huang, Z. (1994). A Mesozoic time scale. *J. Geophys. Res.*, 99, B12, 24051-24074.

Hofmann, A. W. (1988). Chemical differentiation of the Earth: the relationship between mantle, continental crust, and oceanic crust. *Earth Planet. Sci. Lett.*, 90, 297-314.

Kano, K. I. (1989). Interactions between andesitic magma and poorly consolidated sediments: examples in the Neogene Shirahama Group, Sotuh Izu, Japan. *J. Volc. Geotherm. Res.*, 37, 59-75.

Kokelaar, B. P. (1982). Fluidization of wet sediments during the emplacement and cooling of various igneous bodies. *J. Geol. Soc. London*, 139, 21-33.

— (1986). Magma-water interactions in subaqueous and emergent basaltic volcanism. *Bull. Volcanol.*, 48, 275-289.

Kretz, R. (1983). Symbols for rock-forming minerals. *Amer. Mineral.*, 68, 277-279.

Lago, M. (1980). Estudio geológico, petrológico, geoquímico y de aprovechamiento industrial de rocas ofíticas en el Norte de España. *Ph. D. Thesis.*, Univ. Zaragoza, 444 pages.

Lago, M., and Pocovi, A. (1982). Nota preliminar sobre la presencia de estructuras fluidales en las ofitas del área de Estopiñán (provincia de Huesca). *Acta Geol. Hispánica*, 17, 227-233.

Lago, M., and Pocovi, A. (1984). Aspectos geológicos y petrológicos de las doleritas triásicas (ofitas) de Cantabria. *I.º Congr. Esp. Geología*, II, 161-176.

Leake, B. E. (1971). On aluminous and edenitic amphiboles. *Miner. Mag.*, 38, 389-407.

IMA (Leake, B. E., chairman) (1998). Nomenclature of amphiboles: report of the subcommittee on amphiboles of the International Mineralogical Association Commission on new minerals and mineral names. *Miner. Mag.*, 61, 295-321.

Leterrier, J., Maury, R. C., Thonon, P., Girard, D., and Marchal, M. (1982). Clinopyroxene composition as a method of identification of the magmatic affinities of paleovolcanic series. *Earth Planet. Sci. Letter*, 59, 139-154.

Martínez, M. B. (1982). Influencia del substrato en la estructura de la cobertera deslizada de las Sierras Marginales del Prepirineo de Huesca. *Acta Geol. Hispánica*, 17, 235-240.

Martínez Peña, M. B., and Pocovi, A. (1988). El amortiguamiento frontal de la estructura de la cobertera surpirenaica y su relación con el anticlinal de Barbastro-Balaguer. *Acta Geol. Hispánica*, 23, 81-94.

Middlemost, E. A. K. (1975). The basalt clan. *Earth Sci. Rev.*, 11, 337-364.

Montigny, B., Azambre, B., Rossy, M., and Thuziat, R. (1983). Etude K/Ar du magmatisme basique lié au Trias supérieur des Pyrénées. Conséquences méthodologiques et paléogeographiques. *Bull. Minéral.*, 105, 673-680.

Morata, D. (1993). *Petrología y geoquímica de las ofitas de las zonas externas de las Cordilleras Béticas*. Tesis Doctoral, Universidad de Granada, 307 pages.

Sun, S. S., and McDonough, W. F. (1989). Chemical and isotopic systematics of oceanic basalts: implications for mantle composition and processes. In: *Magmatism in ocean basins* (Saunders, A. D., and Norry, M. J., eds.), Geol. Soc. London, Spec. Pub., 42, 313-345.

Tomkeieff, S. I. (1983). *Dictionary of Petrology*. John Wiley & Sons, 680 pp.

Walgenwitz, F. (1976). *Etude pétrologique des roches intrusives triasiques, des écailles du socle profond et des gîtes de chlorite de la région d'Elizondo (Navarre espagnole)*. Thèse 3.e Cycle, Université de Besançon, 172 pages.

Winchester, J. A., and Floyd, P. A. (1973). Geochemical magma type discrimination: application to altered and metamorphosed basic igneous rocks. *Earth Planet. Sci. Lett.*, 28, 459-469.

Recibido el 27 de noviembre de 1999.
Aceptado el 14 de marzo de 2000.